THE APPLICATION OF A PIPE RING EXPANSION TECHNIQUE IN THE FRACTURE TESTING OF A PIPELINE STEEL

M.N.Balsara, L.M.Braga, H.J.MacGillivray† and M.Karam *

The pipe ring expansion technique is an alternative for the fracture testing of pipeline material. Three flawed rings cut from British Gas API standard 5LX grade X65 seam welded steel pipeline were pressurised to various stages of failure. The tests were instrumented to monitor mouth opening displacement, the onset of crack growth, local strains and global strains. The ring expansion technique was able to produce crack growth and failure in the pipe ring sections. Test results seem to support the ability of the British Standards Institute PD6493 to predict maximum load instability but question the validity of the initiation predictions.

INTRODUCTION

Pipelines have been used in the transportation of natural gas for over two decades. The best suited test to assess the integrity of flawed gas pipelines is on full scale sections of pipe. Such tests have been carried out in the past (1) but have proved to be physically difficult to set up and have presented experimental difficulties, both in execution and interpretation. On the other hand, conventional laboratory tests do not represent the real life situation satisfactorily, since flattening of the pipe material implies reduction of ductility and cutting flat samples from the material reduces the thickness with respect to the original pipe wall, in a regime where fracture behaviour is known to be thickness dependent.

In the pipe ring test, a short section of pipe (i.e. a ring) is cut and notched along its length simulating an external axial part-through thickness flaw. A ring expansion rig is used for application of internal pressure to the ring. This paper discusses the experimental aspects of the ring expansion test. The results of the tests are analysed using a level 3 assessment from the British Standards Institute PD6493 (2).

EXPERIMENTAL DETAILS

Ring Expansion Rig

An overall view of the pipe ring expansion rig is shown in figure 1.

† Imperial College of Science, Technology and Medicine, London, U.K.
* Engineering Research Station (ERS), British Gas Plc., Killingworth, U.K.

The pipe ring is placed over a rubber seal which is held between two platens. Oil is used to pressurise the ring via the rubber seal. The seal is slightly longer than the ring and this clearance (about 0.005") ensures that the ring is allowed to expand freely without obstruction during a test. The pressure is applied from a motorised hydraulic pump which allows a variable ramp loading rate.

Three 3" long rings were tested, each cut from a section of the grade X65 pipeline steel. Tests were carried out at the British Gas Engineering Research Station, Killingworth. Each ring was notched along its length using a 0.006" wide slitting saw, with the notch running parallel to the seam weld at 90° around the pipe from the weld. The dimensions of each tested ring are given in table 1. Two rings were pressurised to failure and one up to the onset of crack initiation.

Instrumentation

Pressure was monitored by means of a Bromberg standard test gauge. The loading rate for each test was set to 1psi/min.

A *clip gauge* was used to monitor the mouth opening displacement at the flaw.

Global circumferential expansion was measured by means of a steel tape located around the bottom edge of the ring specimen. One end of the tape is fixed and the free end connected to a displacement transducer.

Local strain was measured at three points around the outer surface of the ring using standard 120Ω strain gauges. The gauges were positioned on the centre line around the ring and were orientated such that hoop strain was measured. The near flaw gauge (gauge 1), positioned 50mm from the edge of the notch, indicated the influence of the flaw on local strains while gauges 2 & 3, one at 90° from the flaw (180° from the weld) and one at 180° from the flaw respectively, measured the nominal hoop strain (see figure 1).

An *alternating current potential drop* (ACPD) system was used to indicate the onset of crack growth. Calibration tests were carried out on small sections of pipe. The stress state seen around the flaw in a pipe ring test was impossible to simulate in the laboratory on a curved section, and instead three-point bend calibration tests were carried out on notched specimens of pipe which were extracted from the CR orientation (thus simulating flaws of the same orientation as in the pipe ring test). Figure 2 gives the nomenclature used for the reference directions in a pipe and correspond with those used by the ASTM. The specimens were loaded up to various stages of failure with the ACPD being monitored during each test. The specimens were then broken open (to see the extent of crack growth, if any) and the resulting calibration curves are shown in figure 3. It is the change of shape of the curves rather than the absolute ACPD values that was used in estimating initiation. Each curve shows a characteristic rise in ACPD as crack tip elastic strains increase and a subsequent drop as plastic strains become dominant. This fall in ACPD continues with crack initiation and subsequent crack growth. The onset of crack initiation in the ring tests was based on calibration curve 2: though crack growth had not started, the presence of crack tip plastic deformation, indicated that initiation was imminent. Consequently, it was estimated in both the calibration tests and pipe ring tests that crack initiation occurred when the ACPD value dropped to 50% of its peak value.

Tensile and Fracture Data - Prior Testing

Earlier testing had concentrated on establishing tensile data and toughness data for the pipeline steel, both of which are necessary when using PD6493. With the

studied flaws being orientated in the axial orientation, the circumferential tensile properties of the pipe were required. Tensile tests were carried out as per ASTM 8M-86a.

The fracture testing was carried out on a series of three-point bend specimens which were extracted from the CR orientation of the pipe, thus simulating the axial part-through thickness flaw seen in the pipe ring tests. The width of each specimen was kept at 13mm (this was the maximum permissible value as specimen width was restricted due to the curvature of the pipe) and thickness varying between 6-12mm. The specimens were side-grooved to simulate the constraint conditions present in the pipe ring specimen. Standard J-type unloading compliance tests were carried out as per ASTM E1152-91.

RESULTS

Tensile Tests. The stress-strain curve characteristics of the pipe material in the circumferential direction are shown in figure 4.

Fracture Testing. The results of the fracture toughness tests are shown in figure 5. An average curve was established and this curve was used as the toughness characteristic curve for the level 3 assessment in PD6493 with the J_{IC} value being estimated at 0.10MN/m.

Pipe Ring Tests. The results from test 1 are summarised in figures 6 & 7. All three tests showed a common variance of potential drop, local strain, global strain, and clip gauge displacement with increasing pressure.

Postulations Using the PD6493 Failure Assessment Diagram (FAD). The results of the level 3 integrity assessment of the postulated flaws are shown in table 1. The assessment analysis for test 1 is shown in figure 8 using the level 3 assessment diagram derived from the tensile test results. The abscissae Lr, defined as the ratio of the net section stress to the material yield strength, was evaluated using the analysis of Willoughby and Davey (3) and the ordinate, Kr, defined as the ratio of the total applied stress intensity factor, K, over the material's failure K was evaluated through the work of Kobayashi et al (4). The pressure locus for the test 1 configuration is shown, the intersection of which with the failure assessment curve gives the predicted initiation pressure as tabulated in table 1. The crack growth locus (tearing locus) for 2mm crack extension is also shown for *that* initiation pressure.

DISCUSSION

1 - Applicability of Ring Expansion Apparatus. The ring expansion technique was able to produce crack growth and failure in a machine notched pipe ring section. In tests 1 & 3, the crack grew in a ductile manner right through the ligament, the micro mechanism being micro-void coalescence. The final 3-4mm of crack growth in each test resulted in shear lip formation as the constraint near the inner diameter reduced. There were no signs of any cleavage fracture in either test.

2 - Strain Gauge Signals. The significance of the local strain around the flaw is shown by the response strain gauge 1 relative to gauges 2 & 3. Gauges 2 & 3, showing the hoop strains on the outside of the pipe, remote from the flaw, give a linear response with pressure as expected. Their values have been checked using

simple stress-strain laws and are in accordance with the nominal hoop stresses in the ring, away from the flaw. The near flaw gauge however shows the effects of bending in the pipe due to the flaw, and local yielding in the ligament. The bending stresses can be separated into two components, namely those due to the internal radial pressure and the curvature of the pipe, and those due to the shift in the bending neutral axis around the flaw.

3 - PD6493 Postulated Results. Figure 8 shows that the crack growth locus in test 1 falls entirely in the 'failure' region of the FAD. Consequently, it is postulated that crack initiation and maximum load instability occur at the same pressure i.e. once a crack has initiated, it will immediately grow through the ligament in an unstable manner. This trend is repeated for the ring 2&3 postulations. The FAD maximum load instability predictions in table 1 are consequently of the same value as the FAD initiation predictions. If these pressure values are checked against the burst pressures in ring tests 1&3, it is seen that the results are in very close agreement i.e. within 2.0%. It seems therefore that the FAD assessment methods can provide accurate estimations for maximum load instability (or burst pressure) in the pipe, provided the appropriate relationships are used in the evaluation of Kr & Lr.

4 - ACPD Signal. The ACPD interpretations from the ring tests indicate a period of stable crack growth before instability conditions. This is in contrast with the FAD analysis where it is postulated that initiation and instability are one event. It is possible that the response of the ACPD system in the calibration tests was different to the ring tests. However the ductile nature of the tested pipeline steel would seem to indicate some initial ductile crack growth before failure.

CONCLUSIONS

Instrumented pipe ring tests are unique in their way of assessing the integrity of flawed pipelines.

Strain gauging of the pipe ring shows the extent of yielding and bending strains around the flaw.

The PD6493, level 3 assessment method can provide an accurate analysis of the failure pressure in the pipe ring specimens if the appropriate data input is accurate.

Initial PD6493 analysis of the pipe ring configuration predicted crack initiation and maximum load instability to be one event.

An ACPD system was used to predict crack initiation and in contrast to the FAD analysis, predicted a period of stable crack growth after initiation. The accuracy of correlating calibration curves from one specimen geometry to another, needs to be investigated.

ACKNOWLEDGEMENTS

The authors would like to thank British Gas Plc. for sponsorship of this work.

REFERENCES

(1) Fearnehough, G.D., Jude, D.W. and Weiner, R.T., Practical Application of Fracture Mechanics to Pressure Vessel Technology, I.Mech.E., p.156, 1971
(2) Published Document PD 6493:1991, British Standards Institute, 1991
(3) Willoughby, A.A. and Davey, T.G., ASTM STP 1020, pp. 390-409, 1989
(4) Kobayashi, A.S., Maiden, D.E., Simon, B.J. and Iida, S., ASME Paper No. 69-WA/PVP-12

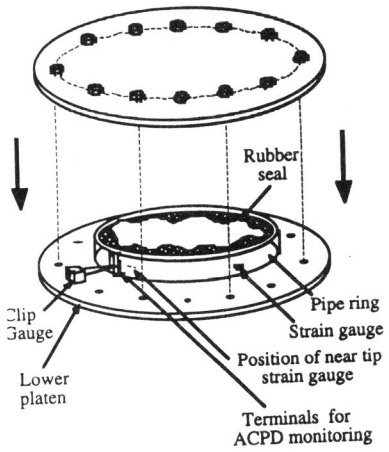

Figure 1 - Overview of Pipe Ring Expansion Apparatus

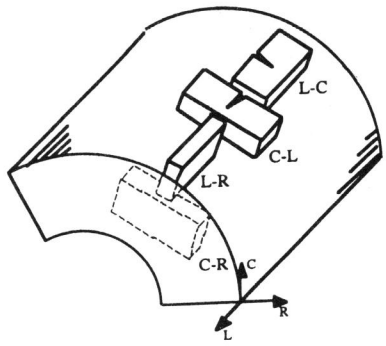

Figure 2 - Nomenclature Used for Pipe Reference Directions

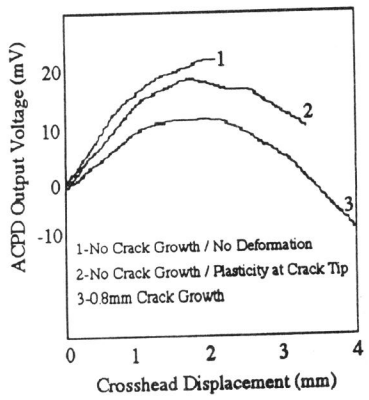

Figure 3 - Potential Drop Calibration Curves

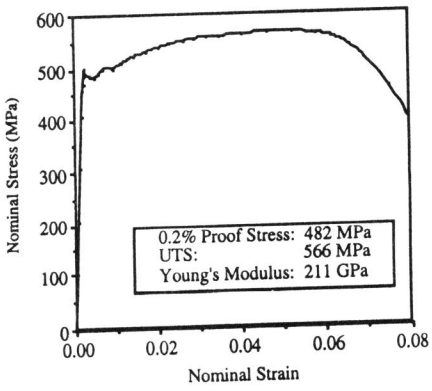

Figure 4 - Circumferential Tensile Properties of X65 Steel

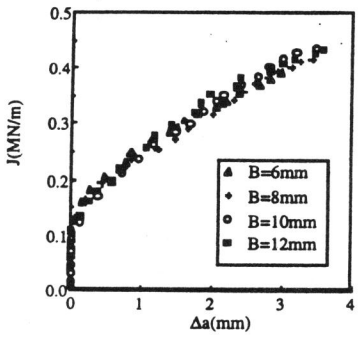

Figure 5 - CR Orientated Fracture Toughness Data

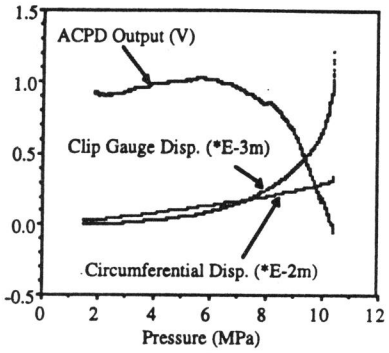

Figure 6 - Test 1 Results; Part I

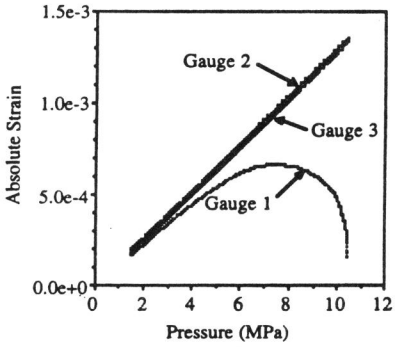

Figure 7 - Test 1 Results; Part II

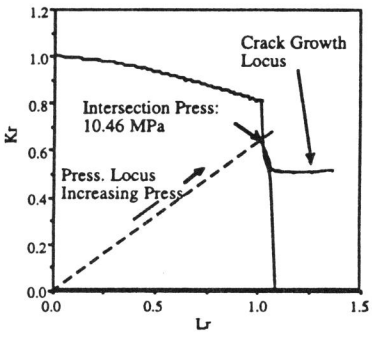

Figure 8 - Test 1, Pressure & Crack Growth Loci; Δa=2mm

Test No.	Level of Failure	Internal Pipe Diameter (mm)	Wall Thickness (mm)	Flaw Depth (mm)	Initiation Pressure From ACPD (MPa)	Max. Load Instability from Test (MPa)	Initiation Pressure From Lev.3 PD6493 (MPa)	Max. Load Instability From Lev.3 PD6493 (MPa)
1	Burst	441.88	15.06	7.2	7.5	10.43	10.46	10.46
2	Initiation	441.88	15.85	7.2	8.8	-	11.44	11.44
3	Burst	441.88	15.45	9.6	5.0	7.60	7.75	7.75

TABLE 1 - Summary of Pipe Ring Tests and Results